

On the Missing Modes When Using the Exact Frequency Relationship between Kirchhoff and Mindlin Plates

C.W. Lim^{1,*}, Z.R. Li¹, Y. Xiang², G.W. Wei³ and C.M. Wang⁴

¹Department of Building and Construction, City University of Hong Kong,
Tat Chee Avenue, Kowloon, Hong Kong

²School of Engineering and Industrial Design & Centre for Construction Technology
and Research, University of Western Sydney, Penrith South DC, NSW 1797, Australia

³Department of Mathematics and Department of Electrical and Computer Engineering,
Michigan State University, East Lansing, MI 48824, U.S.A.

⁴Department of Civil Engineering, National University of Singapore, Kent Ridge,
Singapore 119260

Abstract

An exact frequency relationship exists between Kirchhoff and Mindlin plates of polygonal planform and simply supported edges. In this paper, we show that the use of this relationship leads to missing vibration modes due to the lack of consideration for the transverse shear modes and coupled bending-shear modes in the relationship. The missing modes appear at relatively high order modes and they were originally discovered by using discrete singular convolution (DSC) method that is capable of accurately predicting thousands of vibration modes without suffering from numerical instability as other methods do. An efficient state-space technique is used to confirm our findings. Using the state-space technique, exact vibration frequencies for transverse shear vibration modes of thick plates can be obtained. Numerical examples are presented to support our claims. These exact shear frequencies complement the bending frequencies predicted by using the Kirchhoff-Mindlin relationship. It is interesting to note that there are some coupled bending-shear modes that can be picked up by the DSC method which provides a complete spectrum of frequencies, even for very high frequencies.

Keywords: discrete singular convolution, high frequency, Kirchhoff-Mindlin relationship, transverse shear mode, state-space, thick plate, vibration.

*Corresponding author: C.W. Lim, Department of Building and Construction, City University of Hong Kong, Tat Chee Avenue, Kowloon, Hong Kong, P.R. China. E-mail: bccwlim@cityu.edu.hk

1. Introduction

The Kirchhoff (or classical thin) plate theory [1,2] is the simplest and most commonly used plate theory for bending, vibration and buckling analyses of plates. This theory, however, neglects the effect of transverse shear deformation by the simplified assumption that the normals to the undeformed midplane remain normal after deformation. This theory leads to an overprediction of buckling loads and natural vibration frequencies and an underprediction of deflections when applied to thick plates because of the significant effect of transverse shear deformation in such plates. In 1951, Mindlin [3,4] proposed the first order shear deformation plate theory that relaxes the aforementioned normality assumption. By allowing the straight normals to rotate with respect to the mid-plane of the deformed plate, a constant shear strain is admitted through the plate thickness. This relaxation produces two additional degrees of freedom, i.e. the angles of rotation in the two perpendicular directions, in the plate modeling. Owing to the additional degrees of freedom, various analytical solution methodologies applicable to the Kirchhoff plate analysis become invalid and many exact analyses available in Kirchhoff plate models cannot be extended to the Mindlin (or thick) plate analysis.

In view of the aforementioned problems, Wang and his coauthors [5-9] initiated studies to relate the solutions of Kirchhoff (or thin) plate theory and Mindlin (or thick) plate theory. They derived exact relationships between the two models in bending [5], buckling [6] and vibration [7-9]. Such Kirchhoff-Mindlin relationships exhibit a one-to-one mapping of the exact solutions in both plate models. Consequently many known exact solutions of thin plates can be easily converted to exact thick plate solutions and these exact relationships can be easily handled by practicing engineers who need not have too much knowledge in the thick plate theory.

Nevertheless, there are some inherent pitfalls when using these exact relationships, which is the subject of the present paper. Here, our concern is the missing shear modes in thick plate vibration. As the relationships assume a one-to-one mapping, many physical modes that exist when the thickness of plate becomes relatively high may not be captured. The missing modes are due to transverse shear deformation and coupled bending-shear

deformation in thick plate dynamics. If care is not taken while applying the Kirchhoff-Mindlin relationships, important physical features of the thick plate may not be realized and thus the results may be insufficiently interpreted.

To analyze the missing shear modes, an efficient state-space technique is presented in this paper to derive a system of homogenous differential equation for the vibration of a thick plate considering *only* the transverse shear deformable modes. This method has been shown to be very effective in furnishing exact solutions for bending and vibration of plates and cylindrical shells [10-12]. It is extended here for the analysis of transverse shear vibration modes of thick plates. Exact shear frequency solutions are obtained for plates with two opposite sides simply supported. The exact shear modes complement the bending frequencies predicted from the Kirchhof-Mindlin relationship. However, there are some modes due to the coupling between the bending and the shear dynamics that can not be predicted by the relationship. They can be recovered from the discrete singular convolution (DSC) methods which deliver a complete frequency spectrum for the vibration analysis of thick Mindlin plates. In addition, the influence of plate boundary conditions on the shear vibration frequencies is examined.

The DSC [13-18] method is another potential numerical approach for plate analyses. It is regarded as a novel approach for numerical analysis of singular integrations. The mathematical underpinning of the DSC algorithm is the theory of distributions and wavelet analysis. Many DSC kernels, such as the (regularized) Shannon delta sequence kernel, the (regularized) Dirichlet delta sequence kernel, the (regularized) Lagrange delta sequence kernel and the (regularized) de la Vallée Poussin delta sequence kernel, have been constructed [16]. By appropriately selecting kernel parameters, the DSC approach exhibits controllable accuracy for integration and excellent flexibility in handling complex geometries and boundary conditions. In this paper, a complete spectrum of vibration frequencies is resolved using the DSC collocation (DSC-CO) method and the DSC-Ritz method where the latter is an extension of the Ritz procedure using DSC kernels.

2. Modelling and Formulation

2.1. Problem Definition

Consider an isotropic, elastic, rectangular plate of uniform thickness h , length a , width b , Young's modulus E , shear modulus G , Poisson's ratio ν and mass density ρ , as shown in Fig. 1. The plate is simply supported on two opposite sides and the other two sides may assume free, simply supported or clamped. Here, we intend to determine the vibration frequencies of the plate using three different approaches: (i) the Kirchhoff-Mindlin relationship for bending vibration modes; (ii) the DSC-CO method and the DSC-Ritz method; and (iii) the state-space formulation for shear vibration modes.

2.2. Frequency Relationship of Kirchhoff and Mindlin Plates

The exact frequencies for the vibration of a simply supported, rectangular Kirchhoff (or thin) plate are given by [2]

$$\hat{\omega}_i = \left[\left(\frac{m\pi}{a} \right)^2 + \left(\frac{n\pi}{b} \right)^2 \right] / \sqrt{\rho h / D} \quad (1)$$

where $i = 1, 2, \dots$, corresponds to the mode sequence number and m, n are the number of half number of half waves. The corresponding frequency for a Mindlin plate can be deduced via a formal relationship given by [7,8]

$$\omega_i^2 = \frac{6\kappa^2 G}{\rho h^2} \left\{ \left[1 + \frac{1}{12} \hat{\omega}_i h^2 \sqrt{\frac{\rho h}{D}} \Upsilon \right] - \sqrt{\left[1 + \frac{1}{12} \hat{\omega}_i h^2 \sqrt{\frac{\rho h}{D}} \Upsilon^2 \right] - \frac{\rho h^2}{3\kappa^2 G} \hat{\omega}_i^2} \right\} \quad (2)$$
$$\Upsilon = \left(1 + \frac{2}{\kappa^2 (1 - \mu)} \right)$$

where ω_i correspond to the frequency a Mindlin plate of the same dimensions and material properties, and κ^2 is the shear correction factor.. From Eq. (2), accurate frequencies for a simply supported Mindlin plate can be derived from the Kirchhoff plate solutions given by Eq. (1). These are the flexural vibration modes where a one-to-one mapping between the Kirchhoff plate and the Mindlin plate is possible.

2.3. DSC-Ritz and DSC-CO Formulation

Let T denotes a singular kernel and $\eta(x)$ be an element of the space of test functions. A singular convolution is defined as

$$F(t) = (T * \eta)(t) = \int_{-\infty}^{+\infty} T(t-x)\eta(x)dx \quad (3)$$

where t indicates the time variable and x a dummy variable. Depending on the form of the kernel T , the singular convolution is the key issue for a wide range of problems in science and engineering, e.g., Hilbert transform, Abel transform, and Radon transform. However singular kernels cannot be directly applied in computers because they are tempered distributions and do not have a value anywhere. Hence, the singular convolution in Eq. (3) is of little direct numerical merit. In order to avoid the difficulty of using singular expressions directly in computer, we need to construct sequences of approximations (T_α) to the distribution T

$$\lim_{\alpha \rightarrow \alpha_0} T_\alpha(x) \rightarrow T(x), \quad (4)$$

where α_0 is a generalized limit. Obviously, for the singular kernels of the delta type, $T(x) = \delta(x)$, each element in the sequence, $T_\alpha(x)$, is a delta sequence kernel. With a sufficiently smooth approximation, it is useful to consider a discrete singular convolution (DSC)

$$F_\alpha(t) = \sum_k T_\alpha(t-x_k)f(x_k) \quad (5)$$

where $F_\alpha(t)$ is the approximation of $F(t)$ and $\{x_k\}$ is an appropriate set of discrete points on which the DSC in Eq. (5) is well defined. Note that, the original test function $\eta(x)$ is replaced by $f(x)$.

As the Fourier transform of the delta distribution is unit in the Fourier domain, the distribution can be regarded as a *universal reproducing kernel* [13]

$$f(x) = \int \delta(x-x')f(x')dx' \quad (6)$$

As a consequence, delta sequence kernels are approximate reproducing kernels or bandlimited reproducing kernels that provide a good approximation to the universal reproducing kernel in certain frequency bands.

There are many delta sequence kernels arising in the theory of partial differential equations, Fourier transforms, signal processing and wavelet analysis, with completely

different mathematical properties. For the purpose of numerical computations, the delta sequence kernels of both (i) positive type and (ii) Dirichlet type are of particular importance and they have very distinct mathematical and numerical properties.

For simplicity, we focus on two typical kernels of the Dirichlet type, Shannon's delta sequence kernel

$$\delta_\alpha(x) = \frac{\sin(\alpha x)}{\pi x} \quad (7)$$

and a simplified de la Vallée Poussin delta kernel

$$\delta_\alpha(x) = \frac{1}{\pi\alpha} \frac{\cos(\alpha x) - \cos(2\alpha x)}{x^2} \quad (8)$$

to realize the proposed DSC method.

According to the theory of distributions, the smoothness, regularity and localization of a tempered distribution can be improved by a function of the Schwartz class. It is suggested in [19] that a *delta regularizer* $R_\sigma(x)$ is used in regularizing a delta kernel. A good example is the Gaussian

$$R_\sigma(x) = e^{-\frac{x^2}{2\sigma^2}} \quad (9)$$

Therefore, Shannon's delta sequence kernel in Eq. (7) and de la Vallée Poussin delta kernel in Eq. (8) can be modified in their regularized form as

$$\delta_{\sigma,\alpha}(x) = \frac{\sin(\alpha x)}{\pi x} e^{-\frac{x^2}{2\sigma^2}} \quad (10)$$

and

$$\delta_{\sigma,\alpha}(x) = \frac{1}{\pi\alpha} \frac{\cos(\alpha x) - \cos(2\alpha x)}{x^2} e^{-\frac{x^2}{2\sigma^2}} \quad (11)$$

These regularized kernels converge extremely fast when used for approximating functions and their derivatives. For practical computational purposes, they can be truncated for a finite domain.

For different implementations of the DSC algorithm, the two popular methods are the

Ritz method and the collocation formulation. The DSC-collocation is a local method, in which the derivative of a function at a particular point in the coordinate domain is computed by as a few neighborhood grid points. While the Ritz method is classically a global method, it requires the full set of grid points in a computational domain to compute a derivative. However, the DSC-Ritz can be formulated as a local method because the DSC kernels have time-frequency localization.

The Ritz approach to the Mindlin plate vibration problem is based on the energy principle. By assuming a set of admissible trial functions with independent amplitude coefficients, a closer upper bound for the frequency could be achieved by minimizing the energy functional with respect to the coefficients. In the DSC-Ritz method, a new set of trial functions is employed, which is able to approximate the deflection of the whole domain and at the same time satisfies the prescribed boundary conditions. These trial functions are formed from the product of sets of two-dimensional localized DSC kernels and basic functions which associate the piecewise boundary geometric expressions. The new shape functions φ_k^α ($\alpha = w, \theta_x, \theta_y$) can be expressed as

$$\varphi_k^\alpha(\xi, \eta) = f_k(\xi, \eta)\varphi_l^\alpha \quad (12)$$

where φ_b^α is the basic function. The two-dimensional DSC kernel $\sum_{k=1}^M f_k(\xi, \eta)$ are given

by

$$\sum_{k=1}^M f_k(\xi, \eta) = \sum_{i=1}^N \sum_{j=1}^N \delta_{\sigma ij}(\xi, \eta) \quad (13)$$

where N is the number of grid points adopted in both ξ -direction and η -direction, and

$$M = N^2, \quad k = (i - 1) \times N + j \quad (14)$$

Note that $\delta_{\sigma ij}$ in Eq. (13) is a DSC delta kernel and the two-dimensional forms for the aforementioned two DSC kernels in Eqs. (10-11) can be constructed by tensor products as

$$\delta_{\sigma ij}(\xi, \eta) = \frac{\sin[(\pi / \Delta)(\xi - \xi_i)]\sin[(\pi / \Delta)(\eta - \eta_j)]}{(\pi^2 / \Delta^2)(\xi - \xi_i)(\eta - \eta_j)} e^{-[(\xi - \xi_i)^2 / 2\sigma^2]} e^{-[(\eta - \eta_j)^2 / 2\sigma^2]} \quad (15)$$

for Shannon's kernel, and

$$\delta_{\sigma ij}(\xi, \eta) = \frac{\cos[(\pi/\bar{\Delta})(\xi - \xi_i)] - \cos[(2\pi/\bar{\Delta})(\xi - \xi_i)]}{[(\pi/\bar{\Delta})(\xi - \xi_i)]^2} e^{-[(\xi - \xi_i)^2/2\sigma^2]} + \frac{\cos[(\pi/\bar{\Delta})(\eta - \eta_j)] - \cos[(2\pi/\bar{\Delta})(\eta - \eta_j)]}{[(\pi/\bar{\Delta})(\eta - \eta_j)]^2} e^{-[(\eta - \eta_j)^2/2\sigma^2]} \quad (16)$$

for de la Vallée Poussin kernel. In all the above kernels, ξ_i and η_j are grid point along the ξ -axis and η -axis, respectively. The parameters σ and $\bar{\Delta}$ are chosen as $\sigma = r\Delta$; $\bar{\Delta} = \frac{3}{2}\Delta$, where Δ is the grid spacing, and r is an adjustable parameter determining the radius of influence. Details on how to accommodate the geometric boundary conditions are given by Lim et al. [18, 20, 21].

For the DSC-CO method, the solution of the Mindlin plate vibration problem is obtained by directly solving the discretized partial differential equations. In the DSC-CO, the approximate solution is sought from a finite set of N DSC kernel functions. Numerically to solve the plate vibration governing equation, it is necessary to give a matrix approximation to the differential operator so that the action of the operator can be realized. The DSC approximation to the n th order derivative of a function φ^α ($\alpha = w, \theta_x, \theta_y$) can be rewritten as

$$\frac{\partial^n \varphi^\alpha}{\partial q^n} \Big|_{q=q_k} = \sum_{l=k-M}^{k+M} c_{kl,B}^n \varphi^\alpha \quad (17)$$

where $c_{kl,B}^n$ are a set of DSC weights and can be calculated through the DSC kernel, and q is the direction of differentiation ($q = \xi, \eta$), and n ($= 0, 1, 2, \dots$) is the order of differentiation. The regularized Shannon kernel is used in the present work. By substituting Eq. (17) into the governing differential equations, a system of linear algebraic equations for the governing equations can be obtained. Before calculating the eigenvalues, appropriate boundary conditions are to be implemented. The reader is referred to Refs. [15] and [16] for an elaboration about the DSC-CO method and its applications.

2.4. Exact Solution for Shear Vibration of Thick Plates

Considering only the magnitude of vibration where the time dependent function $\sin \omega t$ has been simplified, the governing differential equations for a thick plate based on the Mindlin plate theory can be expressed as [4]

$$\kappa^2 Gh \left[\frac{\partial}{\partial x} \left(\frac{\partial w}{\partial x} + \theta_x \right) + \frac{\partial}{\partial y} \left(\frac{\partial w}{\partial y} + \theta_y \right) \right] + \rho h \omega^2 w = 0 \quad (18)$$

$$D \left[\frac{\partial}{\partial x} \left(\frac{\partial \theta_x}{\partial x} + \nu \frac{\partial \theta_y}{\partial y} \right) \right] + \frac{(1-\nu)D}{2} \left[\frac{\partial}{\partial y} \left(\frac{\partial \theta_y}{\partial x} + \frac{\partial \theta_x}{\partial y} \right) \right] - \kappa^2 Gh \left(\frac{\partial w}{\partial x} + \theta_x \right) + \frac{\rho h^3}{12} \omega^2 \theta_x = 0 \quad (19)$$

$$D \left[\frac{\partial}{\partial y} \left(\frac{\partial \theta_y}{\partial y} + \nu \frac{\partial \theta_x}{\partial x} \right) \right] + \frac{(1-\nu)D}{2} \left[\frac{\partial}{\partial x} \left(\frac{\partial \theta_y}{\partial x} + \frac{\partial \theta_x}{\partial y} \right) \right] - \kappa^2 Gh \left(\frac{\partial w}{\partial y} + \theta_y \right) + \frac{\rho h^3}{12} \omega^2 \theta_y = 0 \quad (20)$$

where $\theta_x(x, y)$, $\theta_y(x, y)$ are rotations in the x -axis and y -axis, $w(x, y)$ is the transverse displacement, $D = Eh^3/12(1-\nu^2)$ is the flexural rigidity, ω is the angular frequency, and κ^2 is the shear correction factor.

If the plate vibrates in a shear mode, i.e. $w(x, y) = 0$, the governing differential equations reduce to

$$D \left[\frac{\partial}{\partial x} \left(\frac{\partial \theta_x}{\partial x} + \nu \frac{\partial \theta_y}{\partial y} \right) \right] + \frac{(1-\nu)D}{2} \left[\frac{\partial}{\partial y} \left(\frac{\partial \theta_y}{\partial x} + \frac{\partial \theta_x}{\partial y} \right) \right] - \kappa^2 Gh \theta_x + \frac{\rho h^3}{12} \omega^2 \theta_x = 0 \quad (21)$$

$$D \left[\frac{\partial}{\partial y} \left(\frac{\partial \theta_y}{\partial y} + \nu \frac{\partial \theta_x}{\partial x} \right) \right] + \frac{(1-\nu)D}{2} \left[\frac{\partial}{\partial x} \left(\frac{\partial \theta_y}{\partial x} + \frac{\partial \theta_x}{\partial y} \right) \right] - \kappa^2 Gh \theta_y + \frac{\rho h^3}{12} \omega^2 \theta_y = 0 \quad (22)$$

For a simply supported rectangular plate of side length a and width b , the rotations in Eqs. (21) and (22) can be expressed as

$$\theta_x(x, y) = A \cos \frac{n\pi}{a} x \sin \frac{m\pi}{b} y \quad (23)$$

$$\theta_y(x, y) = B \sin \frac{n\pi}{a} x \cos \frac{m\pi}{b} y \quad (24)$$

where n and m are the number of halfwaves of the vibration mode along the x and y directions, and A and B are unknown coefficients to be determined, respectively. By

substituting Eqs. (23) and (24) into Eqs. (21) and (22), the non-trivial frequency ω can be obtained explicitly and expressed in terms of the non-dimensional frequency parameter λ ($= (\omega b^2 / \pi^2) \sqrt{\rho h / D}$) as follows

$$\lambda = \frac{b^2}{\pi^2 h^2} \sqrt{6(1-\nu) \left(12\kappa^2 + \frac{m^2 \pi^2 h^2}{b^2} + \frac{n^2 \pi^2 h^2}{a^2} \right)} \quad (25)$$

where a/b is the aspect ratio and h/b is the thickness ratio of the plate, respectively.

For a plate with simply supported edges opposite to each other, the state-space technique must be adopted to obtain the exact solutions. Assuming that the two simply supported edges are parallel to the x -axis, the rotations in Eqs. (21) and (22) can be expressed as [22]:

$$\theta_x(x, y) = \phi_x(x) \sin \frac{m\pi}{b} y \quad (26)$$

$$\theta_y(x, y) = \phi_y(x) \cos \frac{m\pi}{b} y \quad (27)$$

where $\phi_x(x)$ and $\phi_y(x)$ are unknown functions to be determined. Equations. (26) and (27) satisfy the simply supported boundary conditions on edges at $y=0$ and $y=b$. By substituting Eqs. (26) and (27) into Eqs. (21) and (22), the following differential equation system can be derived

$$(\boldsymbol{\psi})' = \mathbf{H}\boldsymbol{\psi} \quad (28)$$

where $\boldsymbol{\psi} = [\phi_x \quad (\phi_x)' \quad \phi_y \quad (\phi_y)']^T$, the prime ' represents the derivative with respect to x and \mathbf{H} is a 4×4 matrix with the following non-zero elements:

$$H_{12} = H_{34} = 1 \quad (29)$$

$$H_{21} = \frac{D(1-\nu)(m\pi/b)^2 / 2 + \kappa^2 Gh - \rho h \omega^2 / 12}{D} \quad (30)$$

$$H_{24} = \frac{(m\pi/b)(1+\nu)}{2} \quad (31)$$

$$H_{42} = -\frac{(m\pi/b)(1+\nu)}{1-\nu} \quad (32)$$

$$H_{43} = \frac{D(m\pi/b)^2 + \kappa^2 Gh - \rho h^3 \omega^2 / 12}{[D(1-\nu)/2]} \quad (33)$$

A general solution of Eq. (28) can be obtained as

$$\boldsymbol{\psi} = \mathbf{e}^{Hx} \mathbf{c} \quad (34)$$

where \mathbf{c} is a 4×1 constant vector that can be determined by the boundary conditions of the two edges parallel to the y -axis and \mathbf{e}^{Hx} is the general matrix solution of Eq. (28) [22].

The two edges parallel to the y -axis may have the following prescribed boundary conditions when the shear vibration of the plate is considered

$$M_x = 0, \quad M_{xy} = 0, \quad \text{if the edge is free} \quad (35,36)$$

$$M_x = 0, \quad \theta_y = 0 \quad \text{if the edge is simply supported} \quad (37,38)$$

$$\theta_x = 0, \quad \theta_y = 0 \quad \text{if the edge is clamped} \quad (39,40)$$

where M_x and M_{xy} are bending moment and twisting moment in the plate, respectively, and are defined by

$$M_x = D \left(\frac{\partial \theta_x}{\partial x} + \nu \frac{\partial \theta_y}{\partial y} \right) \quad (41)$$

$$M_{xy} = D \frac{1-\nu}{2} \left(\frac{\partial \theta_x}{\partial y} + \frac{\partial \theta_y}{\partial x} \right) \quad (42)$$

In view of Eq. (34), a homogeneous system of equations can be derived by implementing the boundary conditions of the plate along the two edges parallel to the y -axis [Eqs. (35)-(40)] and is given by

$$\mathbf{K} \mathbf{c} = \mathbf{0} \quad (43)$$

where \mathbf{K} is a 4×4 matrix. The vibration frequency ω may be determined when the determinant of \mathbf{K} in Eq. (26) is equal to zero.

3. Numerical Examples

In this section, a few numerical experiments are designed to illustrate the missing modes when using the Kirchhoff-Mindlin relationship for determining shear related vibration modes.

3.1 Simply supported (SSSS) thick plate

Table 1 shows the dimensionless frequencies obtained using the Kirchhoff-Mindlin relationship, exact shear mode solutions from Eq. (25), DSC-Ritz method and DSC-CO method for a plate with a thickness ratio $h/a=0.1$. Prior to mode-113, the Kirchhoff-Mindlin relationship provides exact mapping with respect to the solutions of DSC-Ritz and DSC-CO indicating that there exist no transverse shear modes in this range. At mode 113 and beyond, the mismatch begins to appear. As shown in Table 1, modes-113 to 115 are pure transverse shear modes corresponding to (0,1), (1,0) and (1,1) for the half-wave numbers denoted by (m,n) . The number of missing modes increases for higher frequencies because the shear effect becomes more and more significant when the wavelength becomes shorter.

Although the mismatch of frequencies only appears from mode-113, it is expected that mismatches occur at much lower modes if the plate is thicker. To prove this prediction, two more examples for the SSSS plate are presented in Tables 2 and 3, in which the thickness ratios are $h/a=0.2$ and 0.25 respectively. Indeed, the transverse shear modes start to appear as low as at mode-27 and mode-18, respectively. It is expected that the transverse shear modes begin to dominate the lower order modes when thickness of the plate is further increased.

It is interesting to note that there exists another class of coupled bending-shear vibration modes involving coupled terms of $w-\theta_x$ or $w-\theta_y$ besides the pure bending and pure transverse shear modes as indicated in Table 1. These modes cannot be predicted by the Kirchhoff-Mindlin relationship because the θ_x or θ_y effects are not considered nor they be predicted by the exact shear mode solutions from Eq. (25) because the flexural effect is not considered. It is also

observed that a complete spectrum of accurate frequency solutions can be furnished by both the DSC-Ritz and DSC-CO methods. The latter method exhibits better accuracy when compared to the exact solutions of the Kirchhoff-Mindlin relationship and the exact shear mode solutions. Therefore, DSC-Ritz and DSC-CO are potential methods for analyzing high frequencies in regions where no exact solution exists or other numerical methods, such as the finite element method, encounter failure. For more information on the high frequency analysis, please refer to Lim et al. [18].

3.2 Other thick plates with two opposite sides simple supported (SFSF and SCSC)

To further illustrate the potential of the DSC-Ritz algorithm, two more examples for thick plates are presented. These are plates with two opposite sides simply supported, while the other two sides may be free (named SFSF plate), or clamped (named SCSC plate). These results are presented in Tables 4 and 5, respectively. Here, the exact Kirchhoff-Mindlin frequency relationships are not available. As there is no explicit analytical solution such as that in Eq. (25) available, the state space technique presented in Sec. 2.4 needs to be employed to obtain numerical shear mode solutions by solving Eq. (43). Matching of the shears modes from the state space technique with the complete frequency spectrum as presented in Tables 4 and 5 may create confusion. However, bearing in mind that the Ritz method always overestimates the vibration frequencies, the matching has been done such that the DSC-Ritz solutions are always a little higher than the state space solutions. The pure transverse shear modes start to appear at mode-38 and mode-30, respectively, for the SFSF and SCSC plates. These examples, again, clearly demonstrate that pure shear vibration modes do exist and any exact relationships linking the Kirchhoff and Mindlin plates, if available in the future, must be implemented in care.

To help understand the physical nature of pure shear vibration modes, two examples are presented in Figs. 2 and 3 for a square simply supported plate with $a/b=1$, $h/b=0.1$, $n=3$, $m=2$ (for Fig. 2) and $m=3$ (for Fig. 3), respectively. As observed, these vibration modes only involve deformation in planes parallel to the mid-plane of the plate caused by shear deformation or rotation of the normals originally perpendicular to the

mid-plane. It is also obvious that such modes vibrate at a lower frequency if the plate is thicker.

4. Conclusions

This paper addresses the missing vibration modes of thick Mindlin plates when using a Kirchhoff-Mindlin frequency relationship. The relationship, valid for simply supported and polygonal plates, gives a one-to-one mapping of vibration frequencies between a Kirchhoff plate and a Mindlin plate. It has been served as a useful and convenient tool for analyzing complicated thick plates based on the simple thin plate theory. However, the limitation of such a relationship has not been detected previously. As the Kirchhoff plate accounts only for the bending effect, the transverse shear dynamics is neglected and it plays an important role in the frequency spectrum of Mindlin plates. The pure shear modes are predicted by a state-space technique and are found to complement the bending modes predicted by the relationship. The state-space technique is capable of providing exact frequency parameters for the Mindlin plates. A complete and accurate vibration spectrum of the thick Mindlin plates, including the modes due to bending, shear, and their coupling, are obtained by using discrete singular convolution (DSC) methods, with which the missing modes were original discovered. Numerical examples are designed to support the present claim. Further findings include the fact that the pure transverse shear modes and mode coupling between shear and bending enter into the lower order mode ranges as the thickness of the Mindlin plate increases.

Acknowledgement

This research is supported in part by a Young/Junior Scholars (YSS) Funding of the City University of Hong Kong. The authors wish to thank Dr Yibao Zhao for providing the DSC-CO results.

References

1. Timoshenko SP, Woinowsky-Krieger S. *Theory of plates and shells*, 2nd ed., McGraw-Hill: New York, 1959.
2. Leissa AW. *Vibration of plates*. NASA SP-160, Scientific and Technical Information Office, NASA: Washington DC, 1969.
3. Reissner E. The effect of transverse shears deformation on the bending of elastic plate. *Journal of Applied Mechanics* 1945; 12:69-76.
4. Mindlin RD. Influence of rotary inertia and shear in flexural motion of isotropic, elastic plates. *Journal of Applied Mechanics* 1951; 18:1031-1036.
5. Wang CM, Reddy JN and Lee KH. *Shear Deformable Beams and Plates: Relationships with Classical Solutions*, Elsevier: Singapore, 2000.
6. Reddy JN, Wang CM. Relationship between classical and shear deformation theories on axisymmetric circular plates. *AIAA Journal* 1997; 35: 1862-1868.
7. Wang CM. Natural frequencies formula for simply supported Mindlin plates. *Journal of Vibration and Acoustics* 1994; 116:536-540.
8. Liew KM, Wang CM, Xiang Y, Kitipornchai S. *Vibration of Mindlin Plates: Programming the p-Version Ritz Method*. Elsevier: Oxford, 1998.
9. Wang CM. Vibration frequencies of simply supported polygonal sandwich plates via Kirchhoff solutions. *Journal of Vibration and Vibration* 1996; 190:255-260.
10. Xiang Y, Wang CM. Exact buckling and vibration solutions for stepped rectangular plates. *Journal of Sound and Vibration* 2002; 250:503-517.
11. Xiang Y, Wang CM, Kitipornchai S. Exact buckling solutions for rectangular plates under intermediate and end uniaxial loads. *Journal of Engineering Mechanics*, ASCE, 2003, 129:835-838.
12. Xiang Y, Ma YF, Kitipornchai S, Lim CW, Lau CWH. Exact solutions for vibration of cylindrical shells with intermediate ring supports. *International Journal of Mechanical Sciences* 2002, 44:1907-1924.
13. Wei GW. Discrete singular convolution for the solution of the Fokker-Planck equations. *Journal of Chemical Physics* 1999; 110:8930-8942.
14. Wei GW. Wavelets generated by the discrete singular convolution kernels. *Journal of Physics A* 2000; 33: 8577-8596.
15. Wei GW. Vibration analysis by discrete singular convolution. *Journal of Sound and Vibration* 2001; 244:535-553.
16. Wei GW, Zhao YB, Xiang Y. Discrete singular convolution and its application to the analysis of plates with internal supports. I Theory and algorithm. *International Journal for Numerical Methods in Engineering* 2002;55: 913-946.
17. Xiang Y, Zhao YB, Wei GW. Discrete singular convolution and its application to the analysis of plates with internal supports. II Complex supports. *International Journal for Numerical Methods in Engineering* 2002;55:947-971.
18. Lim CW, Li ZR and Wei GW, DSC-Ritz method for high-mode frequency analysis of thick shallow shells, *I. J. Num. Meth. Eng.*, in press, 2004.
19. Wei GW, Zhang DS, Kouri DJ, Hoffman DK. Lagrange distributed approximating functionals. *Physical Review Letters* 1997; 79:775-779.
20. Liew KM, Lim CW. A Ritz vibration analysis of doubly-curved rectangular shallow shells using a refined first-order theory. *Computer Methods in Applied Mechanics and Engineering* 1995; 127:145-162.

21. Liew KM, Lim CW. Vibration studies on moderately thick doubly-curved elliptic shallow shells. *Acta Mechanica* 1996; 116:83-96.
22. Xiang, Y, Wei, GW. Exact solutions for buckling and vibration of stepped rectangular Mindlin plates. *International Journal of Solids and Structures* 2004; 41:279-294.

Table 1. Comparison of frequency parameter $\lambda = \omega a^2 \sqrt{\rho h / D} / \pi^2$ for an SSSS thick square Mindlin plate with $\nu = 0.3$ and $h/a = 0.1$. Values in parenthesis indicate the mode sequence number corresponding to Kirchhoff-Mindlin relationship [8].

Mode number	Kirchhoff-Mindlin Relationship (mode number)	Exact solutions for pure transverse Shear modes (m,n)	DSC-Ritz Method		DSC-CO Method
			Shannon	de la Vallée Poussin	
113		65.986873 (0,1)	65.99147	65.99128	65.98687
114		65.986873 (1,0)	65.99147	65.99128	65.98687
115		66.308539 (1,1)	66.31618	66.31588	66.30854
116	66.40795 (113)		66.4089	66.40887	66.40795
117	66.40795 (114)		66.4089	66.40887	66.40795
118		†	66.90946	66.90935	66.90818
119		66.947234 (0,2)	66.95178	66.95159	66.94723
120		66.947234 (2,0)	66.9518	66.95161	66.94723
121		67.264307 (1,2)	67.27201	67.27169	67.26431
122		67.264307 (2,1)	67.27201	67.27169	67.26431
123	66.90818 (115)		67.4063	67.4062	67.40523
124	67.40523 (116)		67.4063	67.4062	67.40523
125	67.40523 (117)		67.99322	67.99293	67.98586
126		68.206684 (2,2)	68.21485	68.21448	68.20668
127		68.517929 (0,3)	68.52245	68.52226	68.51793
128		68.517929 (3,0)	68.52245	68.52226	68.51793
129	68.63428 (118)		68.63531	68.63526	68.63428
130	68.63428 (119)		68.63531	68.63526	68.63428
131		68.827767 (1,3)	68.83507	68.83477	68.82777
132		68.827767 (3,1)	68.83509	68.83479	68.82777
133	68.87782 (120)		68.87882	68.87881	68.87782
134	68.87782 (121)		68.87882	68.87881	68.87782
135	68.87782 (122)		68.87903	68.87894	68.87782
136	68.87782 (123)		68.87903	68.87894	68.87782
137	69.60402 (124)		69.60501	69.605	69.60402
138	69.60402 (125)		69.60501	69.605	69.60402
139		69.749023 (2,3)	69.75644	69.7561	69.74902
140		69.749023 (3,2)	69.75644	69.7561	69.74902
141		70.658268 (0,4)	70.6627	70.66251	70.65827
142		70.658268 (4,0)	70.6627	70.66251	70.65827
143	70.79996 (126)		70.801	70.80098	70.79996
144	70.79996 (127)		70.801	70.80098	70.79996
145		70.958761 (1,4)	70.96594	70.96564	70.95876
146		70.958761 (4,1)	70.96594	70.96564	70.95876
147		†	71.25152	71.25118	71.24405
148		†	71.25152	71.25118	71.24405
149		71.257987 (3,3)	71.26393	71.26364	71.25799
150	71.27344 (128)		71.27445	71.2744	71.27344
151	71.27344 (129)		71.27445	71.2744	71.27344
152	71.50916 (130)		71.5103	71.51019	71.50916
153	71.50916 (131)		71.5103	71.51019	71.50916
154		71.852700 (2,4)	71.86011	71.85975	71.85270
155		71.852700 (4,2)	71.86012	71.85976	71.85270
156	72.44531 (132)		72.44637	72.44634	72.44531
157	72.44531 (133)		72.44637	72.44634	72.44531
158	72.44531 (134)		72.44644	72.44635	72.44531
159	72.44531 (135)		72.44644	72.44635	72.44531
160		73.318381 (0,5)	73.32277	73.32258	73.31838
161		73.318381 (5,0)	73.32277	73.32258	73.31838
162		73.318381 (3,4)	73.32415	73.32383	73.31838
163		73.318381 (4,3)	73.32415	73.32383	73.31838
164		73.608015 (1,5)	73.615	73.61471	73.60802

165		73.608015 (5,1)	73.61501	73.61472	73.60802
166	74.28650 (136)		74.28758	74.28751	74.28383
167	74.28650 (137)		74.28758	74.28751	74.28650
168		†	74.29105	74.29071	74.28650
169		74.470159 (2,5)	74.47725	74.47691	74.47016
170		74.470159 (5,2)	74.47725	74.47691	74.47016
171	74.51383 (138)		74.51494	74.5149	74.51383
172	74.51383 (139)		74.51494	74.5149	74.51383
173	75.19217 (140)		75.19322	75.19327	75.19217
174	75.19217 (141)		75.19322	75.19327	75.19217
175		75.322435 (4,4)	75.32798	75.32764	75.32244
176	75.86514 (142)		75.86615	75.86605	75.86514
177	75.86514 (143)		75.8662	75.86624	75.86514
178	75.86514 (144)		75.8662	75.86625	75.86514
179		75.885302 (3,5)	75.89045	75.89017	75.88530
180		75.885302 (5,3)	75.89045	75.89017	75.88530
181			76.21535	76.21509	76.20993
182			76.21535	76.21509	76.20993
183	76.31086 (145)		76.31205	76.31194	76.31086
184	76.31086 (146)		76.31205	76.31194	76.31086
185		76.444024 (0,6)	76.44825	76.44807	76.44402
186		76.444024 (6,0)	76.44825	76.44807	76.44402
187		76.721860 (1,6)	76.7286	76.72832	76.72186
188		76.721860 (6,1)	76.7286	76.72832	76.72186
189	76.97513 (147)		76.97622	76.97618	76.97513
190	76.97513 (148)		76.97622	76.97618	76.97513
191	76.97513 (149)		76.97623	76.97626	76.97513
192	76.97513 (150)		76.97623	76.97626	76.97513
193		77.549393 (2,6)	77.5563	77.55596	77.54939
194		77.549393 (6,2)	77.5563	77.55596	77.54939
195	77.63435 (151)		77.63535	77.63528	77.63435
196	77.63435 (152)		77.63535	77.63528	77.63435
197		77.823283 (5,4)	77.82798	77.82767	77.82328
198		77.823283 (4,5)	77.82798	77.82767	77.82328
199	78.50561 (153)		78.50669	78.50672	78.50561
200	78.50561 (154)		78.50669	78.50672	78.50561
⋮	⋮	⋮	⋮	⋮	⋮
300	91.04199(201)		91.04315	91.04314	91.04199
⋮	⋮	⋮	⋮	⋮	⋮
400		102.382482 (8,9)	102.38756	102.38732	102.38248
⋮	⋮	⋮	⋮	⋮	⋮
500		112.483209 (0,14)	112.48587	112.48572	112.48321
⋮	⋮	⋮	⋮	⋮	⋮
600	121.22680(341)		121.22764	121.22767	121.22680
⋮	⋮	⋮	⋮	⋮	⋮
700	129.88891(386)		129.8955	129.8966	129.88891
⋮	⋮	⋮	⋮	⋮	⋮
800		137.969949 (11,15)	137.974	137.9745	137.96995
⋮	⋮	⋮	⋮	⋮	⋮
900		145.622823 (6,19)	145.62743	145.62784	145.62282
⋮	⋮	⋮	⋮	⋮	⋮
1000		152.475053 (11,18)	152.48328	152.48439	152.47505

† Coupled bending-transverse shear ($w-\theta_x$ or $w-\theta_y$) vibration modes

Table 2. Comparison of frequency parameter $\lambda = \omega a^2 \sqrt{\rho h / D} / \pi^2$ for an SSSS thick square Mindlin plate with $\nu = 0.3$ and $h/a = 0.2$. Values in parenthesis indicate the mode sequence number corresponding to Kirchhoff-Mindlin relationship [8].

Mode number	Kirchhoff-Mindlin Relationship (mode number)	Exact solutions for pure transverse shear modes (m,n)	DSC-Ritz Method	
			Shannon	De la Vallée Poussin
1	1.76791 (1)		1.76895	1.76868
2	3.86562 (2)		3.86660	3.86635
3	3.86562 (3)		3.86660	3.86635
4	5.58787 (4)		5.58870	5.58849
5	6.60060 (5)		6.60107	6.60094
6	6.60060 (6)		6.60107	6.60094
7	7.97367 (7)		7.97419	7.97405
8	7.97367 (8)		7.97419	7.97405
9	9.60179 (9)		9.60207	9.60198
10	9.60179 (10)		9.60207	9.60198
11	9.98018 (11)		9.98063	9.98051
12	10.70825 (12)		10.70856	10.70846
13	10.70825 (13)		10.70856	10.70846
14	12.38760 (14)		12.38793	12.38783
15	12.38760 (15)		12.38793	12.38783
16	12.70297 (16)		12.70324	12.70316
17	12.70297 (17)		12.70324	12.70316
18	13.61439 (18)		13.61469	13.61460
19	13.61439 (19)		13.61469	13.61460
20	14.47946 (20)		14.47971	14.47963
21	15.03345 (21)		15.03380	15.03370
22	15.03345 (22)		15.03380	15.03370
23	15.83408 (23)		15.83422	15.83419
24	15.83408 (24)		15.83422	15.83419
25	16.60199 (25)		16.60214	16.60211
26	16.60199 (26)		16.60214	16.60211
27		16.73681 (0,1)	16.73881	16.73834
28		16.73681 (1,0)	16.73881	16.73834
29	16.85131 (27)		16.85160	16.85151
30	16.85131 (28)		16.85160	16.85151
31		17.05167 (1,1)	17.05373	17.05319
32		17.66457 (0,2)	17.66647	17.66602
33		17.66457 (2,0)	17.66647	17.66602
34	17.81836 (29)		17.81857	17.81852
35	17.81836 (30)		17.81857	17.81852
36		17.96318 (1,2)	17.96531	17.96475
37		17.96318 (2,1)	17.96531	17.96475
38		†	18.57278	18.57230
39		18.83061 (2,2)	18.83329	18.83259
40	18.96628 (31)		18.96652	18.96646
41	18.96628 (32)		18.96652	18.96646
42	18.96628 (33)		18.96663	18.96653
43		19.11101 (0,3)	19.11283	19.11240
44		19.11101 (3,0)	19.11283	19.11240
45		19.38735 (1,3)	19.38913	19.38866
46		19.38735 (3,1)	19.38913	19.38866
47	19.40859 (34)		19.40876	19.40871
48	19.40859 (35)		19.40876	19.40871
49	19.62640 (36)		19.62664	19.62658
50	19.62640 (37)		19.62664	19.62658
51		20.19370 (2,3)	20.19573	20.19519
52		20.19370 (3,2)	20.19573	20.19519

53	20.68451 (38)		20.68479	20.68471
54	20.68451 (39)		20.68479	20.68471
55		20.96906 (0,4)	20.97068	20.97030
56		20.96906 (4,0)	20.97068	20.97030
57		21.22122 (1,4)	21.22285	21.22242
58		21.22122 (4,1)	21.22285	21.22242
59		†	21.23530	21.23475
60		†	21.23530	21.23475
61	21.29650 (40)		21.29674	21.29667
62	21.29650 (41)		21.29674	21.29667
63		21.47042 (3,3)	21.47130	21.47102
64		21.96034 (2,4)	21.96232	21.96179
65		21.96034 (4,2)	21.96232	21.96179
66	22.08838 (42)		22.08862	22.08855
67	22.08838 (43)		22.08862	22.08855
68	22.08838 (44)		22.08862	22.08861
69	22.08838 (45)		22.08862	22.08861
70	22.66560 (46)		22.66584	22.66582
71	22.66560 (47)		22.66584	22.66582
72		23.13980 (0,5)	23.14056	23.14030
73		23.13980 (3,4)	23.14056	23.14030
74		23.13980 (4,3)	23.14135	23.14097
75		23.13980 (5,0)	23.14135	23.14097
76		23.36854 (1,5)	23.37010	23.36969
77		23.36854 (5,1)	23.37010	23.36969
78	23.41477 (48)		23.41492	23.41488
79		†	23.50419	23.50367
80	23.59861 (49)		23.59887	23.59884
81	23.59861 (50)		23.59887	23.59884
82	23.78113 (51)		23.78143	23.78134
83	23.78113 (52)		23.78143	23.78134
84		24.04174 (2,5)	24.04361	24.04312
85		24.04174 (5,2)	24.04361	24.04312
86		24.69658 (4,4)	24.69724	24.69699
87	24.84997 (53)		24.85018	24.85015
88	24.84997 (54)		24.85018	24.85015
89		†	24.87110	24.87086
90		†	24.87110	24.87086
91		25.12367 (3,5)	25.12429	25.12409
92		25.12367 (5,3)	25.12429	25.12409
93	25.19680 (55)		25.19703	25.19700
94	25.19680 (56)		25.19703	25.19700
95		25.54361 (0,6)	25.54492	25.54460
96		25.54361 (6,0)	25.54492	25.54460
97	25.70880 (57)		25.70900	25.70894
98	25.70880 (58)		25.70900	25.70894
99	25.70880 (59)		25.70902	25.70899
100	25.70880 (60)		25.70902	25.70899

† Coupled bending-transverse shear ($w - \theta_x$ or $w - \theta_y$) vibration modes

Table 3. Comparison of frequency parameter $\lambda = \omega a^2 \sqrt{\rho h / D} / \pi^2$ for an SSSS thick square Mindlin plate with $\nu = 0.3$ and $h/a = 0.25$. Values in parenthesis indicate the mode sequence number corresponding to Kirchhoff-Mindlin relationship [8].

Mode number	Kirchhoff-Mindlin Relationship (mode number)	Exact solutions for pure transverse shear modes (m,n)	DSC-Ritz Method	
			Shannon	de la Vallée Poussin
1	1.67251 (1)		1.67339	1.67316
2	3.51237 (2)		3.51313	3.51294
3	3.51237 (3)		3.51313	3.51294
4	4.96330 (4)		4.96392	4.96376
5	5.80103 (5)		5.80138	5.80128
6	5.80103 (6)		5.80138	5.80128
7	6.92403 (7)		6.92441	6.92431
8	6.92403 (8)		6.92441	6.92431
9	8.24174 (9)		8.24194	8.24188
10	8.24174 (10)		8.24194	8.24188
11	8.54634 (11)		8.54667	8.54658
12	9.13100 (12)		9.13122	9.13115
13	9.13100 (13)		9.13122	9.13115
14	10.47380 (14)		10.47404	10.47397
15	10.47380 (15)		10.47404	10.47397
16	10.72524 (16)		10.72545	10.72539
17	10.72524 (17)		10.72545	10.72539
18		10.82537 (0,1)	10.82736	10.82689
19		10.82537 (1,0)	10.82736	10.82689
20		11.13541 (1,1)	11.13743	11.13690
21	11.45088 (18)		11.45110	11.45104
22	11.45088 (19)		11.45110	11.45104
23		11.73094 (0,2)	11.73278	11.73235
24		11.73094 (2,0)	11.73279	11.73235
25		12.01764 (1,2)	12.01969	12.01915
26		12.01764 (2,1)	12.01969	12.01915
27	12.13842 (20)		12.13860	12.13855
28		†	12.56507	12.56462
29	12.57823 (21)		12.57849	12.57842
30	12.57823 (22)		12.57849	12.57842
31		12.83940 (2,2)	12.84193	12.84127
32		13.10187 (0,3)	13.10358	13.10317
33		13.10187 (3,0)	13.10358	13.10317
34	13.21326 (23)		13.21336	13.21333
35	13.21326 (24)		13.21336	13.21333
36		13.35918 (1,3)	13.36084	13.36040
37		13.35918 (3,1)	13.36084	13.36040
38	13.82180 (25)		13.82192	13.82189
39	13.82180 (26)		13.82192	13.82189
40	14.01929 (27)		14.01951	14.01944
41	14.01929 (28)		14.01951	14.01944
42		14.10298 (2,3)	14.10485	14.10435
43		14.10298 (3,2)	14.10485	14.10435
44	14.78493 (29)		14.78509	14.78505
45	14.78493 (30)		14.78509	14.78505
46		14.80947 (0,4)	14.81094	14.81059
47		14.80947 (4,0)	14.81094	14.81059
48		†	14.95788	14.95739
49		†	14.95788	14.95739
50		15.03759 (1,4)	15.03907	15.03868
51		15.03759 (4,1)	15.03907	15.03868
52		15.26231 (3,3)	15.26310	15.26284

53	15.69321 (31)		15.69338	15.69333
54	15.69321 (32)		15.69338	15.69333
55	15.69321 (33)		15.69348	15.69340
56		15.70209 (2,4)	15.70387	15.70339
57		15.70209 (4,2)	15.70387	15.70339
58	16.04305 (34)		16.04318	16.04314
59	16.04305 (35)		16.04318	16.04314
60	16.21531 (36)		16.21549	16.21544
61	16.21531 (37)		16.21549	16.21544
62		16.75110 (0,5)	16.75178	16.75155
63		16.75110 (3,4)	16.75178	16.75155
64		16.75110 (4,3)	16.75248	16.75215
65		16.75110 (5,0)	16.75248	16.75215
66		†	16.93596	16.93550
67		16.95312 (1,5)	16.95450	16.95413
68		16.95312 (5,1)	16.95450	16.95413
69	17.05199 (38)		17.05220	17.05215
70	17.05199 (39)		17.05220	17.05215
71	17.53584 (40)		17.53603	17.53597
72	17.53584 (41)		17.53603	17.53597
73		17.54521 (2,5)	17.54687	17.54644
74		17.54521 (5,2)	17.54687	17.54644
75		†	18.11156	18.11135
76		†	18.11156	18.11135
77		18.11797 (4,4)	18.11855	18.11833
78	18.16187 (42)		18.16202	18.16200
79	18.16187 (43)		18.16202	18.16200
80	18.16187 (44)		18.16205	18.16201
81	18.16187 (45)		18.16205	18.16201
82		18.48996 (3,5)	18.49050	18.49033
83		18.48996 (5,3)	18.49050	18.49033
84	18.61819 (46)		18.61834	18.61832
85	18.61819 (47)		18.61834	18.61832
86		18.85460 (0,6)	18.85574	18.85547
87		18.85460 (6,0)	18.85574	18.85547
88		19.03431 (1,6)	19.03548	19.03517
89		19.03431 (6,1)	19.03548	19.03517
90	19.21044 (48)		19.21056	19.21052
91	19.35578 (49)		19.35595	19.35593
92	19.35578 (50)		19.35595	19.35593
93	19.50008 (51)		19.50030	19.50024
94	19.50008 (52)		19.50030	19.50024
95		19.56352 (6,2)	19.56499	19.56461
96		19.56352 (2,6)	19.56499	19.56461
97		†	19.72642	19.72617
98		†	19.72642	19.72617
99		19.73677 (4,5)	19.73716	19.73701
100		19.73677 (5,4)	19.73716	19.73701

† Coupled bending-transverse shear ($w-\theta_x$ or $w-\theta_y$) vibration modes

Table 4. Comparison of frequency parameter $\lambda = \omega a^2 \sqrt{\rho h / D} / \pi^2$ for an **SFSF** thick square Mindlin plate with $\nu = 0.3$ and $h/a = 0.2$.

Mode number	Pure transverse shear modes via state space method (m,n)	DSC-Ritz Method	
		Shannon	de la Vallée Poussin
1		0.92342	0.92125
2		1.44128	1.43901
3		2.96904	2.96653
4		3.17417	3.17323
5		3.64975	3.64870
6		5.03136	5.02994
7		5.32407	5.32297
8		6.04402	6.04346
9		6.41415	6.41351
10		7.03901	7.03819
11		7.59556	7.59465
12		8.14995	8.14897
13		9.14254	9.14212
14		9.31626	9.31565
15		9.42742	9.42694
16		9.49182	9.49093
17		10.42142	10.42077
18		11.08773	11.08717
19		11.42856	11.42776
20		11.89801	11.89755
21		12.13964	12.13909
22		12.31287	12.31250
23		12.53616	12.53576
24		13.37924	13.37871
25		13.73233	13.73162
26		13.75008	13.74954
27		13.95702	13.95653
28		14.65286	14.65247
29		14.75591	14.75534
30		15.49420	15.49390
31		15.67325	15.67292
32		15.76446	15.76394
33		16.06435	16.06366
34		16.19242	16.19212
35		16.26028	16.25961
36		16.39924	16.39880
37		16.41812	16.41774
38	16.6007 (1,1)	16.73898	16.73859
39		16.84349	16.84314
40	17.05167 (1,2)	17.28252	17.28223
41	17.37767 (2,1)	17.48285	17.48259
42	17.4451 (1,3)	17.50776	17.50743
43	17.52662 (1,4)	17.66688	17.66646
44	17.67456 (2,2)	17.70118	17.70077
45		17.79148	17.79066
46		17.95443	17.95403
47		18.05350	18.05297
48		18.19376	18.19351
49		18.23653	18.23638
50	18.64284 (1,5)	18.66437	18.66405
51	18.64364 (3,1)	18.66604	18.66590
52	18.79337 (3,2)	18.81106	18.81072
53	18.83061 (2,3)	18.92861	18.92798
54		18.94340	18.94316

55	19.0899 (1,6)	19.11263	19.11233
56		19.28849	19.28825
57		19.33888	19.33862
58		19.44614	19.44571
59		19.46583	19.46536
60		19.58656	19.58650
61	19.61604 (2,4)	19.83543	19.83442
62		19.92706	19.92675
63		19.99871	19.99853
64	20.05951 (3,3)	20.42128	20.42095
65	20.27617 (4,1)	20.52665	20.52610
66	20.34318 (4,2)	20.55430	20.55388
67	20.34704 (2,5)	20.77674	20.77641
68	20.39694 (2,6)	20.97049	20.97022
69	20.68835 (1,7)	20.98769	20.98734
70		21.10675	21.10669
71	21.15338 (1,8)	21.22397	21.22368
72		21.24891	21.24875
73		21.30665	21.30606
74		21.35080	21.35077
75	21.47042 (3,4)	21.57703	21.57688
76	21.68637 (4,3)	21.68803	21.68739
77		21.73826	21.73827
78		21.81595	21.81566
79		21.93846	21.93816
80		22.10908	22.10787
81	22.18485 (5,1)	22.18500	22.18477
82	22.20071 (2,7)	22.50202	22.50163
83	22.21188 (5,2)	22.56294	22.56246
84	22.31271 (2,8)	22.56559	22.56554
85		22.65616	22.65592
86		22.78776	22.78762
87	22.85557 (3,5)	23.12547	23.12486
88	23.04663 (4,4)	23.12760	23.12749
89	23.28283 (3,6)	23.14091	23.14072
90		23.20492	23.20479
91		23.36905	23.36875
92		23.37270	23.37266
93	23.40157 (1,9)	23.40455	23.40381
94		23.43693	23.43690
95		23.45869	23.45848
96	23.69095 (5,3)	24.14663	24.14645
97	23.86895 (1,10)	24.30977	24.30970
98	24.30522 (6,1)	24.50793	24.50729
99	24.3153 (6,2)	24.50836	24.50813
100	24.3538 (3,7)	24.54777	24.54629

Table 5. Comparison of frequency parameter $\lambda = \omega a^2 \sqrt{\rho h / D} / \pi^2$ for an SCSC thick square Mindlin plate with $\nu = 0.3$ and $h/a = 0.2$.

Mode number	Pure transverse shear modes via state space method (m,n)	DSC-Ritz Method	
		Shannon	de la Vallée Poussin
1		2.26585	2.26580
2		4.03858	4.03849
3		4.52073	4.52070
4		5.93280	5.93274
5		6.66427	6.66422
6		7.14964	7.14961
7		8.13578	8.13573
8		8.32497	8.32492
9		9.62859	9.62855
10		9.97527	9.97524
11		10.17922	10.17918
12		10.78601	10.78597
13		10.97776	10.97773
14		12.49723	12.49720
15		12.56251	12.56248
16		12.71568	12.71565
17		12.92019	12.92015
18		13.65399	13.65396
19		13.78196	13.78193
20		14.58823	14.58820
21		15.09494	15.09491
22		15.15400	15.15396
23		15.84062	15.84060
24		15.90023	15.90021
25		16.62339	16.62338
26		16.66185	16.66183
27		16.73842	16.73824
28		16.91864	16.91860
29		16.93494	16.93490
30	17.39308 (1,1)	17.46066	17.46060
31	17.52409 (1,2)	17.66610	17.66593
32		17.66921	17.66903
33		17.85399	17.85397
34		17.87033	17.87031
35	18.14919 (2,1)	18.17377	18.17372
36	18.57863 (1,3)	18.84295	18.84282
37		18.92112	18.92108
38		18.97003	18.97000
39		19.02355	19.02350
40		19.11247	19.11230
41		19.14778	19.14766
42	19.15192 (2,2)	19.27029	19.27015
43	19.15888 (1,4)	19.45075	19.45073
44		19.45174	19.45171
45	19.50063 (3,1)	19.51077	19.51075
46		19.63878	19.63875
47		19.72086	19.72079
48	20.34052 (2,3)	20.42864	20.42860
49	20.39963 (2,4)	20.56471	20.56454
50	20.53043 (3,2)	20.70610	20.70607
51	20.65245 (1,5)	20.80752	20.80748
52		20.87142	20.87120
53		20.97037	20.97022
54	21.17176 (1,6)	21.22328	21.22313

55		21.28214	21.28208
56	21.29665 (4,1)	21.30098	21.30096
57		21.33110	21.33107
58		21.33561	21.33558
59	21.95336 (3,3)	22.00132	22.00127
60		22.00182	22.00179
61		22.03818	22.03816
62		22.09068	22.09068
63		22.11550	22.11548
64	22.15998 (2,5)	22.31667	22.31664
65	22.21543 (4,2)	22.36629	22.36614
66	22.36397 (2,6)	22.67315	22.67316
67		22.78245	22.78239
68		22.81254	22.81240
69		23.14105	23.14090
70	23.22768 (3,4)	23.42383	23.42380
71	23.39247 (1,7)	23.44094	23.44078
72	23.42203 (5,1)	23.44174	23.44172
73	23.5859 (4,3)	23.55501	23.55499
74		23.58534	23.58526
75		23.58780	23.58775
76		23.61222	23.61222
77		23.76348	23.76344
78		23.80820	23.80816
79	23.88916 (1,8)	24.26471	24.26468
80	24.23338 (5,2)	24.61324	24.61307
81	24.32951 (3,5)	24.71388	24.71383
82	24.36559 (2,7)	24.84076	24.84074
83	24.51644 (3,6)	24.86787	24.86787
84		24.93749	24.93740
85		25.07021	25.07012
86		25.18142	25.18141
87		25.19828	25.19828
88	25.20483 (2,8)	25.30795	25.30788
89	25.24556 (4,4)	25.47425	25.47423
90	25.48799 (5,3)	25.54466	25.54454
91		25.66224	25.66211
92		25.70990	25.70987
93		25.71361	25.71360
94		25.72961	25.72958
95		25.77838	25.77836
96	25.79071 (6,1)	25.79124	25.79123
97	25.832 (1,9)	25.92834	25.92822
98		26.34634	26.34631
99		26.38597	26.38594
100		26.39584	26.39582

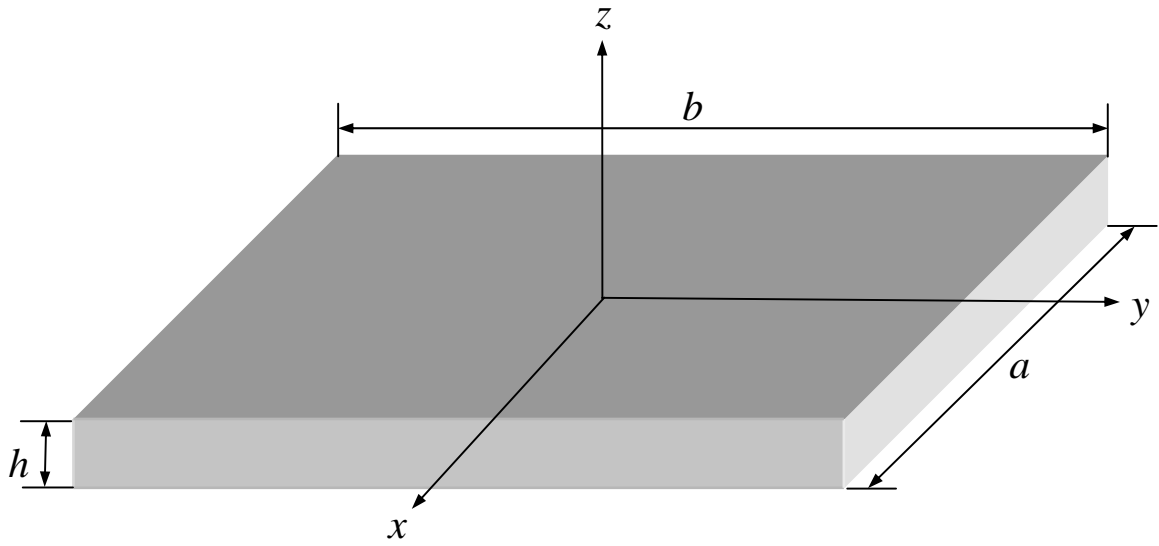


Fig. 1. Geometry of a thick plate.

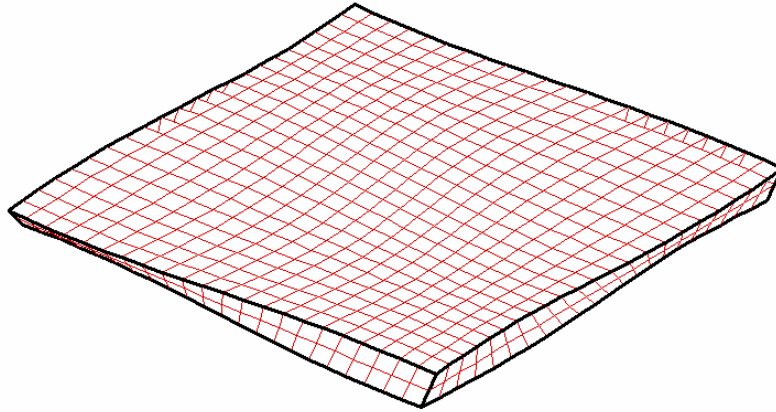


Fig. 2. Pure shear vibration mode for a square simply supported plate with $a/b=1$, $h/b=0.1$, $n=3$, $m=2$ and $\lambda=69.749023$.

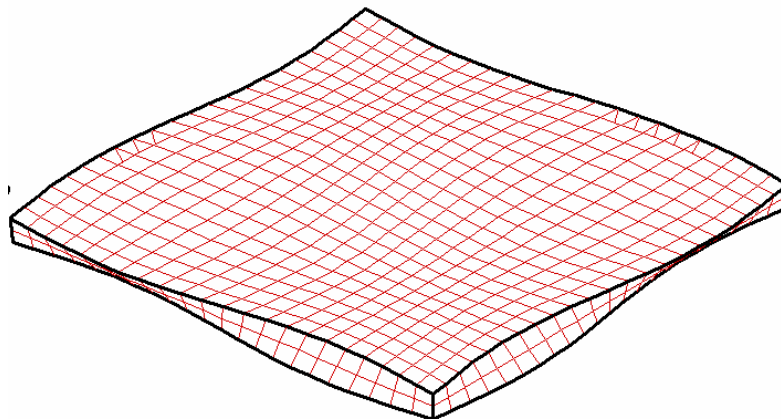


Fig. 3. Pure shear vibration mode for a square simply supported plate with $a/b=1$, $h/b=0.1$, $n=3$, $m=3$ and $\lambda=71.257987$.